Digital Filter Initialization for HIRLAM

Peter Lynch, Ray McGrath and Aidan McDonald

Met Éireann, Dublin

HIRLAM Technical Report No. 42

ABSTRACT

A digital filter initialization scheme has been introduced into the HIRLAM model and compared to the reference implicit normal mode initialization scheme. This report presents details of the scheme and the results of extensive tests showing its advantages. The scheme is shown to be more effective than the reference normal mode initialization scheme in eliminating spurious high frequency noise from the forecasts. In a parallel run using FASTEX data, the scores produced by the DFI run were significantly better than those of the reference run. The advantages of digital filter initialization demonstrated in this report should justify the adoption of the digital filtering initialization scheme as a new reference scheme for HIRLAM.

Digital Filter Initialization for HIRLAM

1. Introduction

The requirement to modify meteorological analyses to avoid spurious high frequency oscillations in numerical forecasts has been known from the beginning of numerical weather prediction. Indeed, it was the omission of this crucial step which led to the completely unrealistic result for pressure tendency obtained by Richardson (1922). The spurious oscillations are caused by gravity wave components of large amplitude, resulting primarily from minor errors in the observations.

The most popular method of initialzation up to recently was the normal mode method (Machenhauer, 1977). This has been used in many NWP centres, and has performed satisfactorily. Its most natural context is for global models, for which the horizontal structure of the normal modes corresponds to the Hough functions, the eigenmodes of the Laplace Tidal Equations. For limited area models, normal modes can also be derived, but the lateral boundaries force the introduction of simplifying assumptions. A method equavalent to the normal mode method, called implicit normal mode initialization (INMI), was introduced by Temperton (1988). For INMI it is not necessary to derive the normal modes explicitly; the problem is reduced to the numerical solution of Helmholtz equations. This is the method which is used in the reference HIRLAM model. It is described in Haugen (1992).

For the standard method of implementation of NMI, it is found that the initialization procedure converges only for the modes of largest vertical scale. Therefore, the application of the method is restricted to the first few vertical modes. In HIRLAM with sixteen vertical levels, as used in the study of Haugen (1992), four vertical modes were initialized (`nmodes=4`). The same number of modes are initialized in the current reference system (HIRLAM Version 4.4 has 31 levels but still `nmodes=4`). We note that in the 19 level model at ECMWF five modes were initialzed, and this number was not changed when the 31 level model was introduced. In the present study, a 24 level model is used. The limitation to four vertical modes has the consequence that imbalance at the lower model levels is not removed.

Recently, an alternative method of initialization, called digital filter initialization (DFI), was introduced by Lynch and Huang (1992). It was generalised to allow for diabatic effects by Huang and Lynch (1993). The latter paper also discussed the use of an optimal filter. A much simpler filter, the Dolph-Chebyshev filter, which is a special case of the optimal filter, was applied to the initialization problem by Lynch (1997). A more efficient way of performing the initialization was presented by Lynch, Giard and Ivanovici (1997). The implementation described in this report is based on the last reference.

The method of digital filter initialization, which is based on ideas from digital signal processing, has significant advantages over alternative methods, and is now in use operationally at several major weather prediction centres: NCEP in Washington, NOAA in Boulder, DWD in Offenbach, Météo-France in Toulouse, CMC in Montreal, BMRC in

Melbourne and others. Some of the advantages when compared to available alternatives are:

1: No need to compute or store normal modes

2: No need to separate vertical modes; no ambiguity in pressure/temperature changes

3: Complete compatibility with model discretisation; exotic coordinates and distorted grids cause no problems

4: No iterative numerical procedure which may diverge; therefore, ability to initialize all model vertical modes

5: Ease of implementation and maintenance, due to simplicity of scheme

6: Applicable to all prognostic model variables

7: Applicable to non-hydrostatic models.

The first advantage is shared by INMI. However, the second is not: INMI requires the introduction of an auxiliary geopotential variable, and partitioning of its changes between the temperature and surface pressure involves an *ad hoc* assumption. Advantage 3 facilitates the use of stretched model grids. Advantage 4 means that all the vertical modes can be initialized effectively. The simplicity of the method makes it easy to implement and maintain. Additional prognostic model variables, such as cloud water, rain water, turbulent kinetic energy, etc., are processed in the same way as the standard mass and wind variables. Thus, DFI produces initial fields for these variables which are compatible with the basic dynamcial fields. Finally, for non-hydrostatic models, the additional prognostic variables are filtered in a manner identical to that used for the basic variables. The DFI method is thus immediately suitable for non-hydrostatic models (Bubnová, *et al.*, 1995). This is not the case for normal mode initialization.

It must be pointed out that DFI is significantly more demanding of computational time than normal mode initialization. The version of DFI described in this report requires that an adiabatic hindcast and a diabatic forecast, each of two hours duration, be carried out. Thus, the overhead is roughly equivalent to a three hour forecast. However, the results presented show that there are significant benefits, which justify this additional cost.

In this report a DFI scheme is introduced, and an implementation in the HIRLAM model is described. The report includes technical details of the method of introducing the scheme into the model code. The DFI scheme is compared to the reference INMI scheme. A detailed case study of a particular analysis and forecast is carried out to demonstrate that the DFI scheme performes satisfactorily and indeed is superior to the reference scheme in several important respects. A comprehensive parallel series of forecasts is then carried out and the model scores show that the DFI scheme results in forecasts which are of greater accuracy than those produced by the reference scheme.

2. The Dolph-Chebyshev Filter

The details of the Dolph-Chebyshev filter are presented in Lynch (1997). We will confine the present discussion to the definition and principal properties of the filter;

further information may be found in the reference cited.

The function to be described is constructed using Chebyshev polynomials, defined by the equations

$$T_n(x) = \begin{cases} \cos(n \cos^{-1} x), & \text{if } |x| \leq 1; \\ \cosh(n \cosh^{-1} x), & \text{if } |x| > 1. \end{cases}$$

Clearly, $T_0(x) = 1$ and $T_1(x) = x$. From the definition, the following recurrence relation follows immediately:

$$T_n(x) = 2xT_{n-1}(x) - T_{n-2}(x), \quad n \geq 2.$$

The main relevant properties of these polynomials are given in Lynch (1997).

Now consider the function defined in the frequency domain by

$$H(\theta) = \frac{T_{2M}\left(x_0 \cos\left(\theta/2\right)\right)}{T_{2M}(x_0)}$$

where $x_0 > 1$. Let θ_s be such that $x_0 \cos(\theta_s/2) = 1$. As θ varies from 0 to θ_s, $H(\theta)$ falls from 1 to $r = 1/T_{2M}(x_0)$. For $\theta_s \leq \theta \leq \pi$, $H(\theta)$ oscillates in the range $\pm r$. The form of $H(\theta)$ is that of a low-pass filter with a cut-off at $\theta = \theta_s$. By means of the definition of $T_n(x)$ and basic trigonometric identities, $H(\theta)$ can be written as a finite expansion

$$H(\theta) = \sum_{n=-M}^{+M} h_n \exp(-in\theta).$$

The coefficients $\{h_n\}$ may be evaluated from the inverse Fourier transform

$$h_n = \frac{1}{N}\left[1 + 2r \sum_{m=1}^{M} T_{2M}\left(x_0 \cos\frac{\theta_m}{2}\right) \cos m\theta_n\right],$$

where $|n| \leq M$, $N = 2M + 1$ and $\theta_m = 2\pi m/N$ (Antoniou, 1993). Since $H(\theta)$ is real and even, h_n are also real and $h_{-n} = h_n$. The weights $\{h_n : -M \leq n \leq +M\}$ define the Dolph-Chebyshev or, for short, Dolph filter.

In the HIRLAM model, the filter order $N = 2M + 1$ is determined by the time step Δt and forecast span T_S. The desired frequency cut-off is specified by choosing a value for the cut-off period, τ_s. Then $\theta_s = 2\pi\Delta t/\tau_s$ and the parameters x_0 and r are given by

$$\frac{1}{x_0} = \cos\frac{\theta_s}{2}, \quad \frac{1}{r} = \cosh\left(2M \cosh^{-1} x_0\right).$$

As the function `cosh` may not be available an alternative, algebraic, expression for r may be used. It is known that, for all x,

$$T_K = \tfrac{1}{2}\left[(x + \sqrt{x^2 - 1})^K + (x - \sqrt{x^2 - 1})^K\right].$$

This may be used to evaluate $r = 1/T_{2M}(x_0)$, as is done in the subroutine `DOLPH`. The ripple ratio r is a measure of the maximum amplitude in the stop-band $[\theta_s, \pi]$:

$$r = \left[\frac{\text{side-lobe amplitude}}{\text{main-lobe amplitude}}\right]$$

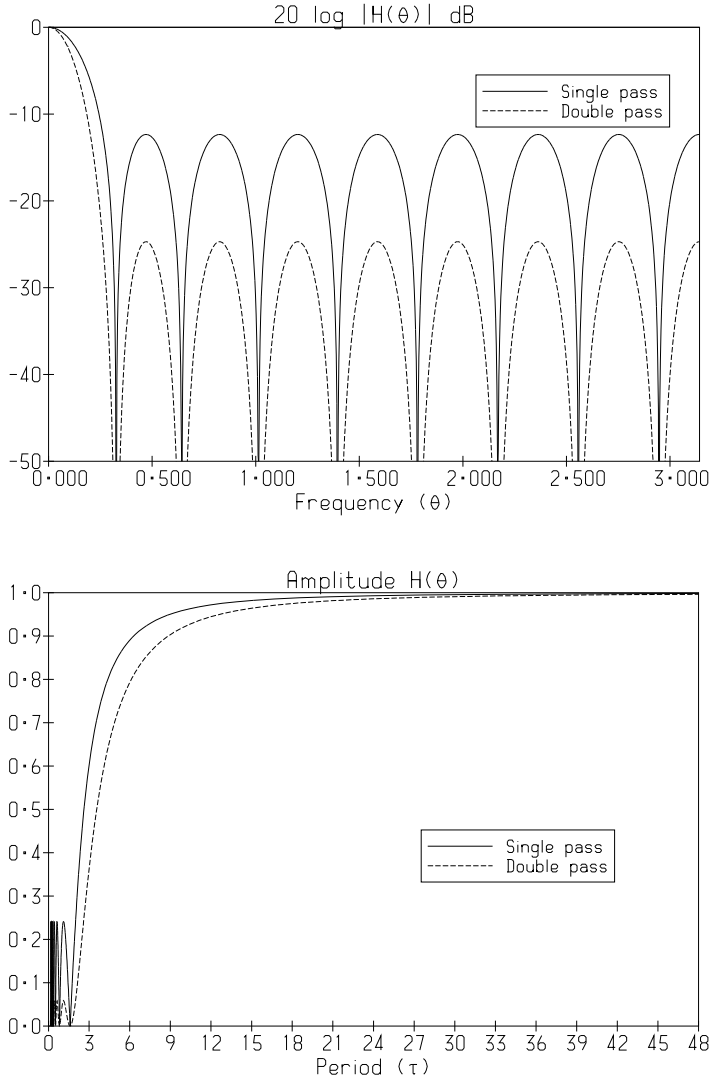

Fig. 1. Frequency response for Dolph filter with span $T_S = 2$h, order $N = 2M + 1 = 17$ and cut-off $\tau_s = 3$h. Results for single and double application are shown. Top: Logarithmic response (dB) as a function of frequency. Bottom: Amplitude response as a function of period.

The Dolph filter has minimum ripple-ratio for given main-lobe width and filter order.

Let us suppose components with period less than three hours are to be eliminated ($\tau_s = 3\,\mathrm{h}$) and the time step is $\Delta t = \frac{1}{2}\,\mathrm{h}$. Then $\theta_s = 2\pi\Delta t/\tau_s \approx 1.05$. It can be shown that a filter of order $N = 7$, or span $T = 2M\Delta t = 3\,\mathrm{h}$, attenuates high frequency components by more than 20 dB (the attenuation in the stop-band is $\delta = 20\log_{10}|H(\theta)|$). This level of damping implies that the amplitudes of high-frequency components are reduced by at least 90% and their energy by at least 99%, which is found to be adequate in practice.

The DFI procedure employed in the HIRLAM model involves a double application of the filter. Thus, we examine both the frequency response $H(\theta)$ and its square, $H(\theta)^2$, as the effect of a second pass through the filter is to square the frequency response. The

parameters chosen for the DFI tests below are span $T_S = 2\,\mathrm{h}$, cut-off period $\tau_s = 3\,\mathrm{h}$ and time step $\Delta t = 450\,\mathrm{s} = \frac{1}{8}\,\mathrm{h}$. So, $M = 8$, $N = 17$ and $\theta_s = 2\pi\Delta t/\tau_s \approx 0.26$. The response and square response are shown in Fig. 1. The ripple ratio has the value $r = 0.241$. A single pass attenuates high frequencies (components with $|\theta| > |\theta_s|$) by at least 12.4dB. For a double pass, the minimum attenuation is about 25dB, more than adequate for elimination of HF noise. For ease of visualisation, the response is also plotted as a function of period in Fig. 1 (bottom panel). From this it is clear that the amplitudes of components with periods less than two hours are reduced to less than 5% of their original value. At the same time, components with periods greater than one day are substantially left unchanged. It is crucial for an initialization scheme that it does not distort the meteorologically significant components of the flow: the filter described here has the required property.

In Lynch (1997, Appendix) it is proved that the Dolph window is an *optimal* filter whose pass-band edge, θ_p, is the solution of the equation $H(\theta) = 1 - r$. Since an optimal filter is, by construction, the best possible solution to minimizing the maximum deviation from the ideal in the pass- and stop-bands, the Dolph filter shares this property provided the equivalence holds. However, note the essential distinction: for the general optimal filter, θ_p can be freely chosen; for the Dolph window, it is determined by the other parameters. The algorithm for the optimal filter is complex, involving about one thousand lines of code; calculation of the Dolph filter coefficients is trivial by comparison.

3. Implementation in HIRLAM

3.1 Practical Procedure

The digital filter initialization is performed by applying the filter to time series of model variables. The coefficients of the Dolph filter, $\{h_n : -M \le n \le +M\}$, are real and symmetric: $h_{-n} = h_n$. Thus, the phase response is such that the output is valid at the centre of the span. If we had a model integration centred on the initial time, $t = 0$, the filter would produce output valid at that time. However, as the model contains irreversible physical processes, it is not possible to integrate it backwards in time. The solution is to apply the filter in two stages: in the first, a backward integration from $t = 0$ to $t = -T_S$ is performed, with all irreversible physics switched off. The filter output is calculated by accumulating sums of the form

$$\bar{x} = \sum_{n=0}^{n=N} h_{n-M} x_n \,,$$

where x is a particular prognostic variable at a particular grid point and level (the same sum is accumulated for all prognostic variables). The output $\bar{x}$ is valid at time $t = -\frac{1}{2}T_S$. In the second stage, a forward integration is made from $t = -\frac{1}{2}T_S$ to $t = +\frac{1}{2}T_S$, starting from the output of the first stage. Once again, the filter is applied by accumulating sums formally identical to those of the first stage. But now the output is valid at the centre of the interval $[-\frac{1}{2}T_S, +\frac{1}{2}T_S]$, *i.e.*, at $t = 0$. The output of the second pass of the filter is the initialized data.

The values of the prognostic variables at the lateral boundaries are left unchanged during the digital filtering process. The boundary value at any particular time is computed from an equation of the form

```
VALUE = FIELD1+TIMRAT*(FIELD2-FIELD1)
```

where `FIELD1` and `FIELD2` are the values at the start and end of the interval for which boundary fields are specified. The maintenance of constant values at the boundaries is arranged by the simple subterfuge of setting the variable `TIMRAT` to zero during DFI. We experimented with the more elaborate procedure of allowing for variation of the boundary values in accordance with the external forcing. However, whilst adding considerably to the complexity of the initialization procedure, this did not lead to any improvement in performance, so the simpler option of constant boundary values was chosen.

3.2 Technical Implementation

The subroutine `GEMINI` required substantial modifications to implement the DFI scheme. A new COMMON block, `COMDFI` was introduced, with control parameters for the DFI scheme and arrays to store the accumulation of the filtered fields. The filtered output fields are accumulated in the arrays `HFT(MLNLT*MLEV)`, `HFU(MLNLT*MLEV)`, `HFV(MLNLT*MLEV)`, `HFQ(MLNLT*MLEV)`, `HFS(MLNLT*MLEV)`, `HFPS(MLNLT)` and `HFLNPS(MLNLT)`. Additional arrays are required to store the analysed values of the prognostic surface fields, *viz.,* soil temperature and humidity and snow; these are `HFTS(MLNLT)`, `HFTD(MLNLT)`, `HFSW(MLNLT)`, `HFSD(MLNLT)` and `HFSN(MLNLT)`. They are unchanged by the DFI procedure, but it is necessary to save their initial values, as they change during the integration. Further changes were made to insure that the cloud water was advected 'backwards' during the adiabatic stage.

The initialization and forecast are performed through the medium of the script `Forecast`. It is modified so as to execute three runs of the model. These are indicated colloquially as a hop, skip and jump.

• **Hop:** The first run is the adiabatic backward integration. The output of this is written to an intermediate file `im{$DTG}00`. Strictly, it is valid at $t = -\frac{1}{2}T_S$, but this is not reflected in the naming since $-\frac{1}{2}T_S$ may be a fraction of an hour; the prefix `im` is a sufficient signal, and the file is used only as input to the next stage.

• **Step:** The second run spans the range $[-\frac{1}{2}T_S, +\frac{1}{2}T_S]$, starting from the intermediate file `im{$DTG}00`. The output is written to the file `in{$DTG}00`. This is the file of initialized data, used to begin the forecast and perhaps also for diagnostic purposes.

• **Jump:** The third run is the normal forecast, covering whatever range is required, typically 48 hours, using `in{$DTG}00` for the initial data.

4. Detailed Case Study

The digital filter initialization (DFI) was implemented both in Version 2.7.15, operational at Met Éireann in early 1999, and in the reference Version 4.3, introduced in March, 1999. A detailed case study based on the first implementation was carried out to check the effect of the initialization on the initial fields and on the forecast, and to examine the efficacy of DFI in eliminating high frequency noise. The digital filter initialization was compared to the reference implicit normal mode initialization (NMI) scheme, and to forecasts with no initilaizaiton (NIL). Forecasts starting from the analysis valid at 1200 UTC on 10 February, 1999 were compared.

```
C-----------------------------------------------------------
C
C            COMMON Block COMDFI
C   COMMON Block for DIGITAL FILTERING.
C
C-----------------------------------------------------------
C
C   Specified Parameters:
C
C    LDFI   Logical variable:
C           If .TRUE. then apply DFI
C           If .FALSE. do not apply DFI
C    NDFI   Indicator for method of filtering
C           = 0 :  No filtering
C           = 1 :  Launching (forward stage only)
C           = 2 :  Full two-stage filtering
C    NFILT  Indicator for filter type
C           = 1 :  Dolph-Chebyshev filter
C    TSPAN  Time-span (seconds) for the adiabatic and
C           diabatic stages of the initialization
C    TAUS   Cutoff period (seconds) for the filter
C           (TAUS is the stop-band edge for the Dolph filter)
C
C   Computed parameters:
C
C    THSBAK  Cutoff frequency THETAS for hindcast stage
C    THSFWD  Cutoff frequency THETAS for forecast stage
C    NBAK    Number of time-steps for adiabatic hindcast
C    NFWD    Number of time-steps for diabatic forecast
C
C   Output of the subroutine DOLPH:
C
C    HDFI(0:NHMAX) Filter coefficients h(n) (NHMAX = 360)
C                  These are held in COMMON Block pardfi.
C-----------------------------------------------------------
C
          LOGICAL LDFI
          INTEGER NDFI, NFILT, NBAK, NFWD
          REAL HDFI, TSPAN, TAUS, DTBAK, DTFWD, THSBAK, THSFWD
C
          INTEGER NHMAX
          PARAMETER (NHMAX = 360)
          COMMON /PARDFI/ HDFI(NHMAX),
         +        LDFI, NDFI, NFILT, TSPAN, TAUS, DTBAK, DTFWD,
         +        THSBAK, THSFWD, NBAK, NFWD
C
C-----------------------------------------------------------
C
C    Fields for accumulation of summations in
C    Digital Filtering Initialization (DFI).
C
C-----------------------------------------------------------
C
          COMMON / COMDFI / HFPS, HFLNPS, HFT, HFU, HFV, HFQ,HFS
         +                , HFTS, HFTD, HFSW, HFSD, HFSN
C
          REAL
         +  HFT(MLNLT*MLEV), HFU(MLNLT*MLEV), HFV(MLNLT*MLEV),
         +  HFQ(MLNLT*MLEV), HFS(MLNLT*MLEV)
         +  HFPS(MLNLT), HFLNPS(MLNLT),
         +  HFTS(MLNLT), HFTD(MLNLT), HFSW(MLNLT),
         +  HFSD(MLNLT), HFSN(MLNLT)
C
C-----------------------------------------------------------
```

Table 1. Changes in model prognostic variables at analysis time and for the 24-hour forecast, induced by digital filtering initialization. Units are SI except for surface pressure (hPa). Maximum and root-mean-square changes are given.

	Winds				Temps			
	Analysis		Forecast		Analysis		Forecast	
Level	max	rms	max	rms	max	rms	max	rms
1	20.4	2.21	.662	.213	1.77	.324	.418	.071
2	14.6	1.53	2.11	.434	.905	.187	.424	.066
3	12.1	1.52	3.45	.513	.726	.163	.707	.085
4	13.5	1.55	4.39	.704	1.30	.189	1.08	.112
5	14.6	1.85	9.90	.995	1.71	.228	1.89	.183
6	17.0	2.05	12.6	1.40	2.75	.272	2.80	.264
7	12.2	2.31	22.4	2.27	2.36	.257	3.88	.251
8	15.2	2.45	21.2	2.61	1.30	.211	1.72	.199
9	14.1	2.38	20.9	2.51	1.57	.189	1.82	.196
10	11.7	2.27	23.2	2.52	1.17	.180	1.69	.196
11	10.9	2.08	19.8	2.36	.887	.182	1.56	.205
12	10.6	1.87	18.8	1.97	1.21	.168	2.06	.186
13	9.37	1.66	12.4	1.61	1.56	.159	1.92	.189
14	7.81	1.45	11.2	1.32	1.44	.156	1.17	.150
15	7.39	1.35	10.7	1.18	1.38	.153	1.25	.152
16	7.36	1.28	11.8	1.03	1.25	.158	1.56	.152
17	7.07	1.25	9.41	.886	1.31	.163	2.12	.172
18	7.97	1.20	6.52	.785	1.69	.179	1.12	.159
19	8.52	1.21	7.23	.680	1.69	.203	2.94	.215
20	11.8	1.34	9.58	.651	1.62	.214	3.19	.189
21	14.7	1.49	11.2	.696	2.00	.259	1.68	.133
22	15.2	1.69	12.1	.708	2.31	.329	1.83	.117
23	13.0	1.95	10.6	.684	2.44	.366	1.84	.116
24	11.8	2.23	8.36	.623	2.75	.416	1.88	.119

Psurf	Analysis		Forecast	
	max	rms	max	rms
	2.21	.493	.924	.110

4.1 Changes induced by DFI

We first checked the effect of DFI on the analysis and forecast fields. The changes to the multi-level wind and temperature fields are given in Table 1. The change in surface pressure is also given. We see that the maximum change in surface pressure is 2.2hPa, with an *rms* change of about 0.5hPa. The changes to the other analysed variables are in general comparable in size to analysis errors, and considerably smaller in magnitude than typical changes brought about by the analysis itself: the *rms* change in surface pressure from first-guess to analysis (not tabulated) is about 1hPa.

Table 1 also gives the impact of DFI on a 24 hour forecast: the *rms* and maximum differences between the uninitialized (NIL) forecast and the filtered (DFI) forecast for all prognostic variables are given. When we compare these values to the differences at the initial time they are seen to be generally smaller. The changes made by DFI are to the high frequency components; since these are selectively damped during the course of the forecast, the two 24 hour forecasts are very similar. Note that the maximum difference in surface pressure is less than 1hPa and the *rms* difference is only 0.1hPa.

The surface fields (soil temperature and humidity) are not changed by DFI. Experiments in which the surface fields *were* filtered produced results which were less satisfactory than those in which they were left unchanged. It is believed that this may be due to a time shift induced by the process: the surface fields are unchanged during the adiabatic, backward stage. But the forward stage advances them in time, with the result that the filtered output does not strictly refer to the analysis time. Since the surface fields are not expected to vary at high frequency, it seems appropriate to preserve the analysed values.

4.2 Impact on Noise Profile

The basic measure of noise is the mean absolute value of the surface pressure tendency

$$N_1 = \left(\frac{1}{\mathrm{NMAX}}\right) \sum_{\mathrm{n}=1}^{\mathrm{NMAX}} \left|\frac{\partial p_s}{\partial t}\right| .$$

For well balanced fields this quantity has a value of about 1 hPa/3h. For uninitialized fields it can be an order of magnitude larger. In Figure 2 we plot the value of N_1 for three forecasts. The solid line represents the forecast from uninitialized data: we see that the value of N_1 at the beginning of the forecast is about 12 hPa/3h, and it takes about six hours to fall to a reasonable value. The dashed line is for a forecast starting from data initialized using the implicit normal mode method (NMI). The starting value is about 3 hPa/3h, falling to about 1.5 hPa/3h after twelve hours. The final graph (the dotted line) is for the digitally filtered data (DFI). The initial value of N_1 is now about 1.5, and remains more-or-less constant throughout the forecast. It is clear from this measure that DFI is more effective in removing high frequency noise than NMI.

4.3 Changes in Surface Pressure

In Fig. 3, the top panel shows the change induced in surface pressure by DFI. As stated above, the maximum change is 2.2hPa, with a root-mean-square change of about 0.5hPa. It is clear that there are no changes at the lateral boundaries. The corresponding difference chart for the 24 hour forecasts starting from the filtered and original analyses (DFI-NIL) is shown in the bottom panel of Fig. 3. The maximum difference is less than 1hPa, in agreement with Table 1, and the *rms* difference is only 0.1hPa. For practical purposes, these forecasts are identical. There is evidence of some small-scale noise in mid-Atlantic. Closer examination of the two forecasts showed that there is some small-scale structure in both. However, it is of quite small amplitude (the contour interval is 0.1 hPa for both plots) and of no synoptic significance.

Comparison of the other fields for the DFI and NIL forecasts confirmed that there were no operationally significant differences between them, with one exception. Examination of the surface temperature and two-metre temperature showed that there were

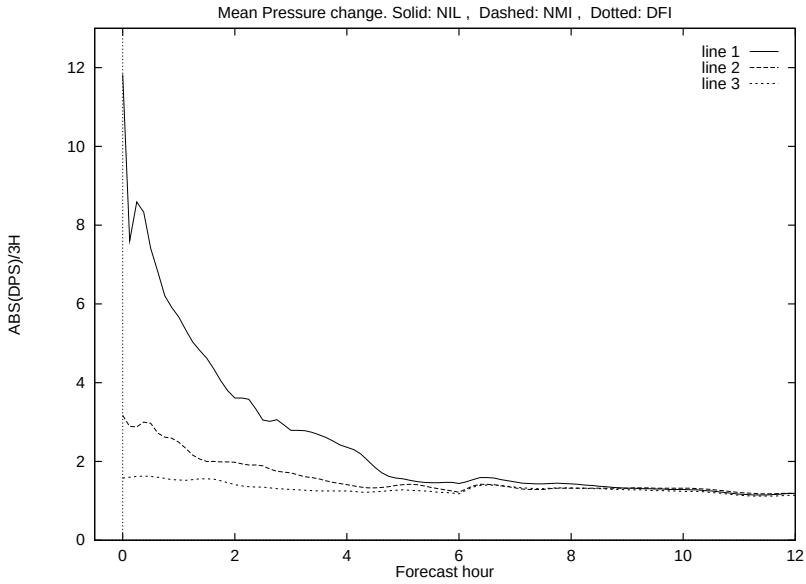

Fig. 2. Mean absolute surface pressure tendency for three forecasts. Solid: uninitialized analysis (NIL). Dashed: Normal mode initialization (NMI). Dotted: Digital filter initialization (DFI). Units are hPa/3 hours.

isolated differences, of small spatial scale, in the 24 hour forecasts, of up to 8°. This is quite surprising, in view of the fact that DFI does not make any changes in the initial surface fields. It transpired that this behaviour, hyper-sensitivity of the surface temperature to very small changes in analysis, has been seen elsewhere, and is believed to be due to a coding error in the treatment of surface variables, which has so far eluded detection. A crude test with Version 2.7 demonstrated this sensitivity: the initial humidity field was everywhere increased by 10%. As a result, changes of up to 6° were seen in the 24 hour forecast. This behaviour has not been reported for HIRLAM Version 4.3, and the offending code may well have been removed or inadvertantly rectified! We are confident that these discrepancies have nothing to do with the digital filtering itself.

4.4 Comparisons with Normal Mode Initialization

We have already seen (Fig. 2) that DFI is more efficient that NMI in eliminating high frequency noise. There are many possible reasons for this, but one primary one is that only four vertical modes are initialized by the INMI scheme. An examination of the changes induced by the normal mode scheme showed that the prognostic variables at the lowest model level were almost unchanged. This is in sharp contrast to the behaviour of DFI. We saw in Table 1 that the changes at level 24 are comparable in size to those at upper levels. Because of the structure of the normal modes, low-level values project predominantly onto the higher-order modes, which are not influenced by NMI. Thus, the changes are small for these variables. This is demonstrated clearly in Table 2: the changes induced in the prognostic model variables by NMI, and the resulting differences in the 24-hour forecast, are shown there. (Adiabatic DFI would give smaller changes, but is less effective in eliminating noise). In general, the changes due to NMI are

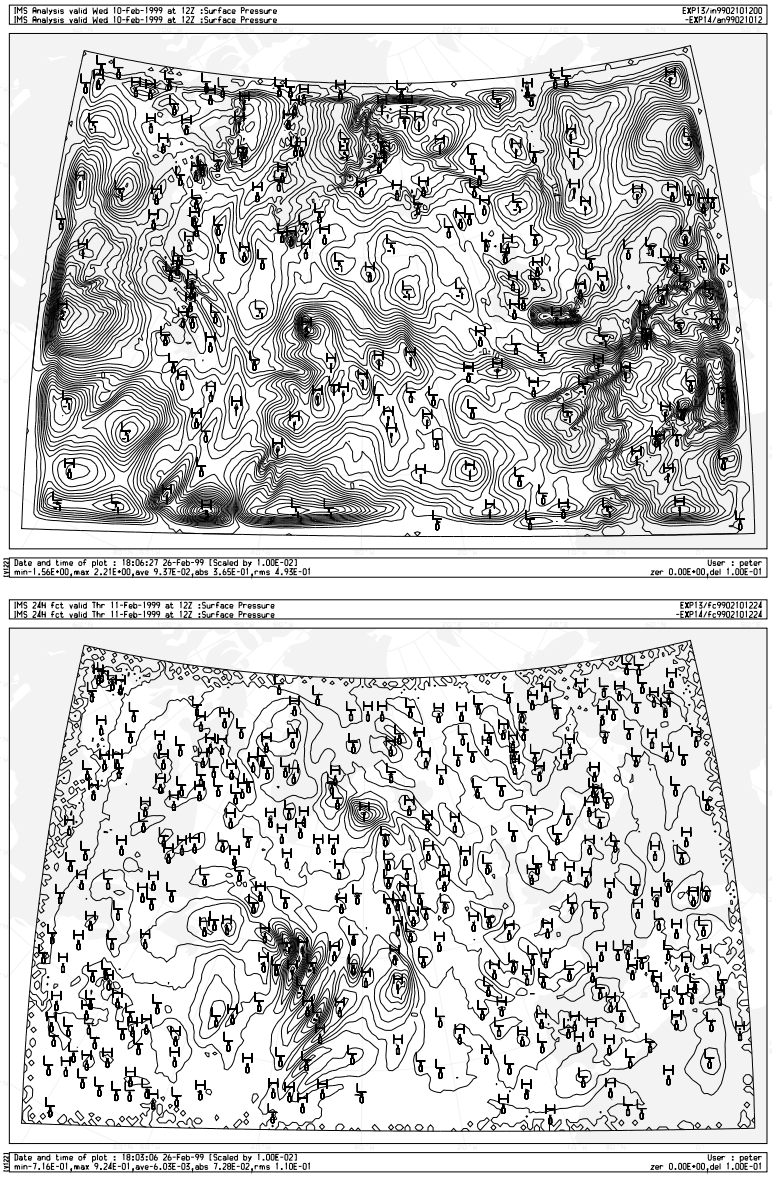

Fig. 3. Top panel: Changes in surface pressure resulting from digital filtering. Bottom panel: Difference in 24 hour forecasts of surface pressure from the DFI analysis and the uninitialized analysis (DFI-NIL). Note that the contour interval is 0.1 hPa for both plots.

comparable to those of DFI, or perhaps somewhat smaller. However, the changes in temperature for the lowest model levels induced by NMI are only a small fraction of those induced by DFI; in fact, they are negligible.

The surface observations must be expected to give rise to significant imbalance in the lower layers. Thus, a sizeable change by the initialization is to be expected if the high frequency gravity wave noise introduced by these observations is to be removed. We conclude that INMI scheme, as currently configured, is quite inefficient in coping with

Table 2. Changes in model prognostic variables at analysis time and for the 24-hour forecast, induced by implicit normal mode initialization. Units are SI except for surface pressure (hPa). Maximum and root-mean-square changes are given.

	Winds				Temps			
	Analysis		Forecast		Analysis		Forecast	
Level	max	rms	max	rms	max	rms	max	rms
1	14.2	2.55	1.45	.415	1.85	.460	.657	.145
2	15.7	2.33	3.19	.991	1.48	.309	.510	.112
3	11.6	1.73	3.71	1.05	1.33	.320	.758	.135
4	12.3	1.56	5.89	1.12	1.20	.274	.924	.140
5	11.6	1.85	10.5	1.28	.828	.173	1.86	.196
6	10.5	1.93	13.5	1.57	.703	.152	3.44	.236
7	9.44	1.81	18.0	2.05	.827	.196	2.40	.205
8	8.37	1.62	15.7	2.17	.860	.237	1.38	.172
9	7.37	1.43	17.7	2.14	.960	.259	1.31	.167
10	6.50	1.29	14.9	2.00	.999	.264	1.94	.166
11	5.78	1.21	14.7	1.79	.984	.257	1.66	.159
12	5.17	1.20	12.3	1.46	.976	.240	1.48	.144
13	4.67	1.22	8.43	1.23	.875	.220	1.22	.141
14	4.93	1.26	8.09	1.06	.750	.195	1.16	.136
15	5.17	1.31	5.52	.924	.688	.170	1.25	.124
16	5.36	1.36	4.78	.828	.562	.145	1.50	.122
17	5.49	1.39	5.20	.773	.438	.122	1.38	.123
18	5.57	1.42	3.76	.697	.375	.100	1.19	.129
19	5.62	1.43	2.46	.616	.312	.083	1.31	.149
20	5.63	1.44	3.49	.601	.250	.066	1.31	.125
21	5.62	1.44	4.46	.613	.250	.060	.971	.091
22	5.60	1.43	5.05	.621	.250	.051	1.13	.084
23	5.57	1.42	4.90	.601	.250	.053	.938	.086
24	5.54	1.42	4.06	.555	.312	.048	1.25	.079

Psurf	Analysis		Forecast	
	max	rms	max	rms
	1.94	.561	.681	.116

gravity wave noise at low levels. It is also to be noted that the default implementation of INMI in HIRLAM is adiabatic. This limits its efficacy unnecessarily: Huang and Lynch (1993) showed convincingly that incorporation of diabatic effects had a significant beneficial effect for a limited area model even in middle latitudes (see their Fig. 6).

We compare the level-24 winds for the three analyses (NIL, NMI and DFI) in Fig. 4. The top panel shows the uninitialized field. It is zoomed in over a region in mid-Atlantic. There is clearly some significant small-scale noise in this field. Examination of the first-guess field (not shown) showed that it was already present there, and since there were few observations in this region, it passed through to the analysis. The centre

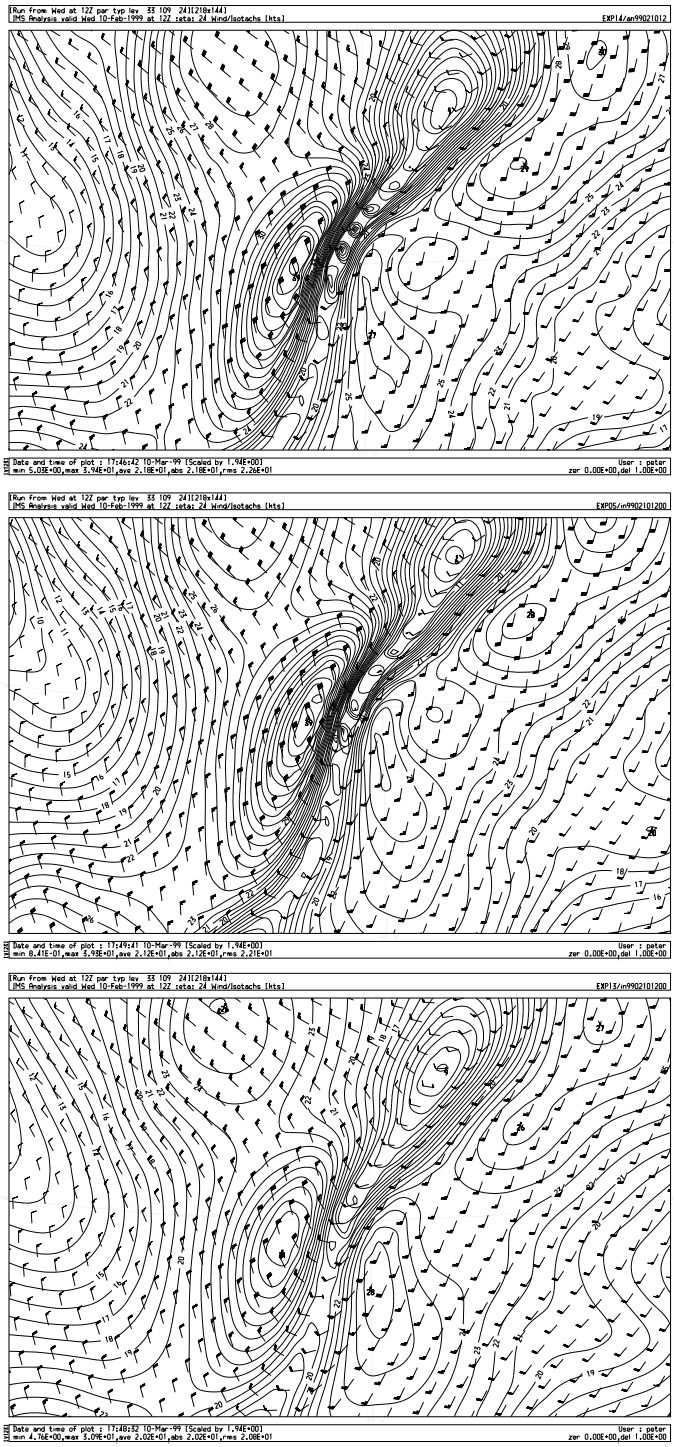

Fig. 4. Wind arrows and isotachs for a region in mid-Atlantic, at the lowest model level (level 24) at the initial time. Top panel: No initialization (NIL); Middle panel: Normal mode initialization (NMI); Bottom panel: digital filter initialization (DFI).

panel shows the field for the NMI case. While there is some slight reduction in the noise, it is still clearly present. The bottom panel shows the DFI wind at level 24. It is clearly much smoother; the small-scale structures have been effectively eliminated. This suggests that DFI is more effective than NMI in dealing with imbalance at low levels.

The measure N_1 indicates the noise in the vertically integrated divergence field. However, even when this is small, there may be significant activity in the internal gravity wave modes. To see this, we look at the vertical velocity field at 500 hPa for the NIL, NMI and DFI analyses. The top panel in Fig. 5 shows the uninitialized vertical velocity field, zoomed in over western Europe and the eastern North Atlantic. There is clearly substantial gravity wave noise in this field. In fact, the field is physically quite unrealistic. The centre panel shows the field for the NMI case. While there is a marked reduction in the noise, there remain unrealistic values over southern Britain and northern France which cannot be linked to any orographic features. The bottom panel shows the DFI vertical velocity. It is much smoother; the spurious features have been eliminated and the large values with small horizontal scales which remain are clearly associated with the Scottish Highlands, the Norwegian Mountains and the Alps. This suggests strongly that DFI is more effective than NMI in dealing with internal gravity wave noise. It is noteworthy that stationary mountain waves are unaffected by digital filtering, since they have zero frequency. This is a desirable characteristic of the DFI scheme.

5. Comprehensive Comparison using FASTEX Data

The detailed case study reported above was done with HIRLAM Version 2.7. The DFI scheme was then implemented in Version 4.3 and a more comprehensive evaluation was undertaken using a FASTEX dataset. The FASTEX analyses covered the period 10–17 February, 1997. Using a 3-hour data assimilation cycle, two sets of forecasts were generated using the DFI and NMI initialization schemes with HIRLAM Version 4.3. In both cases, identical sets of observations were used, and the boundary fields — ECMWF analyses — were identical for both cycles. Forecasts out to 48 hours were produced at 6-hour intervals (there were 30 forecasts for each run). Forecasts were verified against the corresponding analyses and by comparison with the observations. The field verification was over a central area, (40°N — 65°N and 25°W — 10°E).

The results were very encouraging: the forecast skill for the DFI scheme was markedly superior to that of the reference run. Scores were either better than or comparable to those using the reference HIRLAM Version 4.3 with the implicit NMI scheme in its default configuration (`nlinmi=.t., nmodes= 4, nitnmi= 3`).

In Fig. 6 we plot the *rms* and bias errors for mean sea-level pressure as a function of forecast time, averaged over all thirty forecasts. The lines marked with crosses are for the reference run, and those marked with spots are for the DFI run (this convention is used also in Figs. 7 and 8). The *rms* scores are significantly better for DFI, and the improvement is greater for longer forecast times. At 48 hours, there is a reduction in *rms* error of about 0.5hPa, which is substantial, representing an increase in predictive skill of six hours. The bias error (dashed curve) is reduced slightly.

The *rms* and bias errors for 500 hPa temperature are shown in In Fig. 7 (again, averaged over all thirty forecasts). The *rms* scores are again markedly better for DFI than for the reference run. The bias error (dashed curves) is about the same for both runs. Similar improvements in forecast temperature were found at other levels.

Finally, the *rms* error in the vector wind at 300hPa is shown in Fig. 8. Once again, the results clearly favour the DFI scheme: the error is less at all time ranges, being reduced at 48 hours by about 2m/s. Improvements in the wind forecasts were also

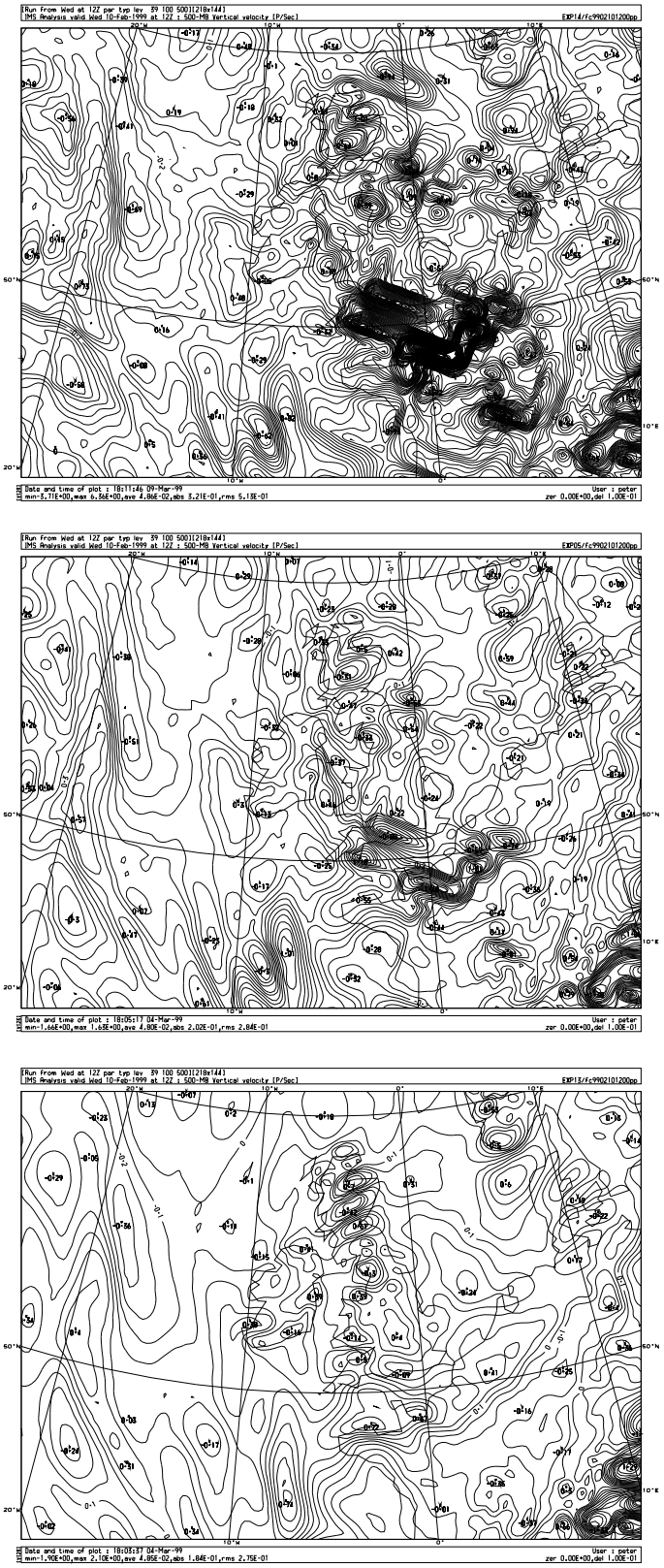

Figure 5. Vertical velocity at 500 hPa over western Europe and the eastern North Atlantic. (Top) Uninitialized analysis (NIL); (middle) after normal mode initialization (NMI); (bottom) after digital filtering (DFI).

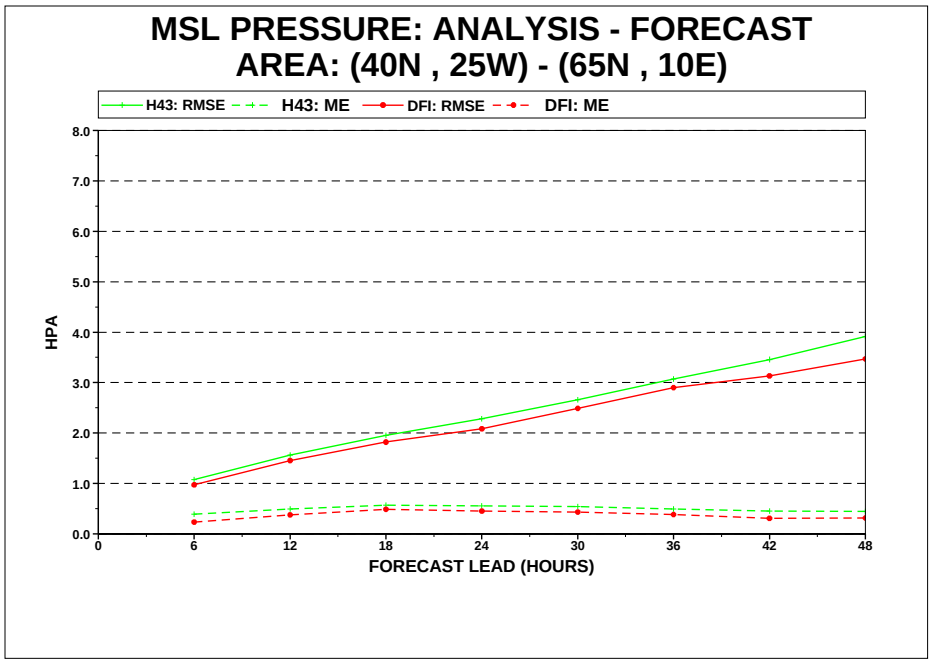

Fig. 6. Root-mean-square (solid) and bias (dashed) errors for mean sea-level pressure, as a function of forecast time, averaged over all thirty forecasts. Lines marked with crosses are for the reference run (NMI); those marked with spots are for the DFI run.

found at other model levels.

Verifications of forecast surface parameters against SYNOP observations were made for stations in Ireland and the UK. Mean sea-level pressure errors were marginally less for DFI than for the reference, but the differences were only a few percent. The differences for $T_{2\mathrm{m}}$ and $V_{10\mathrm{m}}$ were also negligible. We conclude that the impact for the surface parameters is essentially neutral.

As it is not usual for an initialization scheme to yield significant improvements in forecast accuracy, some discussion is merited. We cannot demonstrate beyond question the reason for this improvement. However, the comparative results presented above have shown up come definite defects in the implicit normal mode initialization as implemented in the reference HIRLAM model. It is clear that the NMI scheme is not eliminating imbalance at lower model levels. Moreover, although the noise level indicated by the parameter N_1 falls to a reasonable level in six hours, there may still be internal gravity wave noise which is not measured by this parameter. Any noise in the six hour forecast will be carried through to the next analysis cycle, and will affect the quality control and assimilation of new observational data. It is believed that the DFI scheme, with its superior ability to establish atmospheric balance, results in improved assimilation of data and consequently in a reduction of forecast errors.

6. Summary

A digital filter initialization scheme has been introduced into the HIRLAM model and compared to the reference implicit normal mode initialization scheme. A detailed case

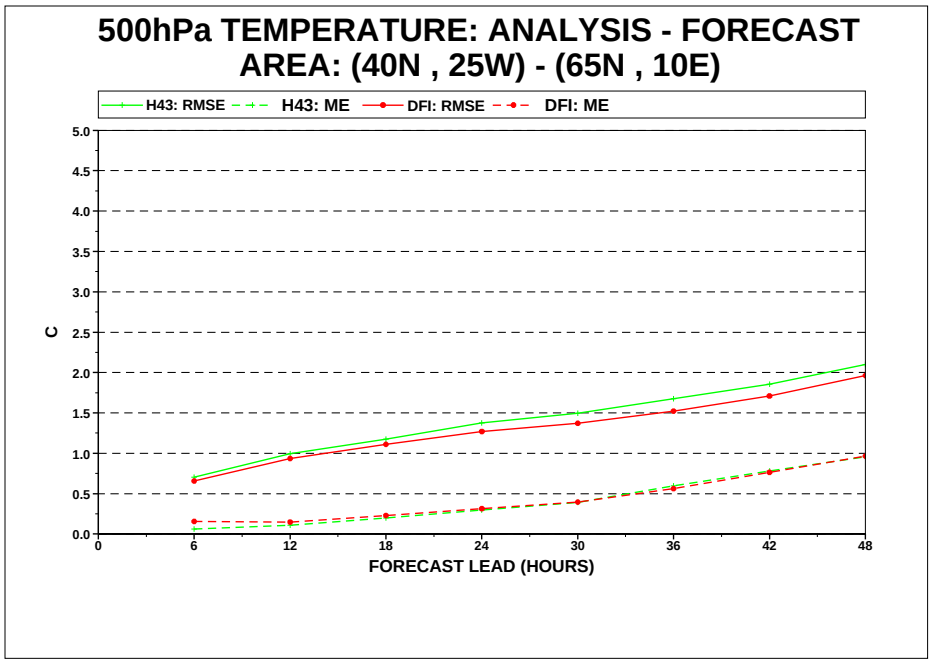

Fig. 7. Same as Fig. 6 but for errors in forecast 500 hPa temperature.

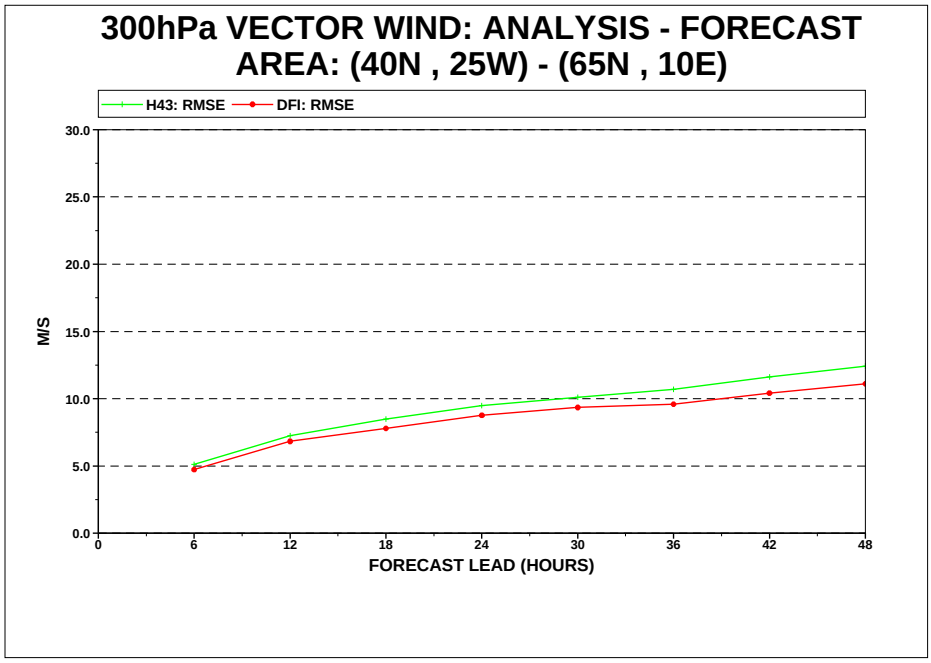

Fig. 8. Similar to Figs. 5 and 6 but for errors in forecast 300 hPa vector wind.

study has shown that the INMI scheme is defective in certain important respects. The DFI scheme was shown to be more effective in eliminating spurious high frequency noise from the forecasts. In a parallel run using FASTEX data, the scores produced by the DFI run were significantly better than those of the reference run.

The DFI scheme has now been implemented in the MPP code, HIRLAM Version 4.4, and tested satisfactorily. Thus, it is ready for use as the default initialization method.

The clear advantages shown in this report should justify the adoption of the digital filtering initialization scheme as a new reference scheme for HIRLAM.

Acknowledgement

The authors are most grateful to Xiang-Yu Huang, DMI, for reviewing this report.

References

Antoniou, A, 1993: *Digital Filters: Analysis, Design and Applications.* 2nd Edn., McGraw-Hill, 689pp.

Bubnová, Radmila, Gwenaëlle Hello, Pierre Bénard and Jean-François Geleyn, 1995: Integration of the fully elastic equations cast in the hydrostatic pressure terrain-following coordinate in the framework of the ARPEGE/Aladin NWP system. *Mon. Wea. Rev.*, **123**, 515–535.

Dolph, C.L., 1946: A current distribution for broadside arrays which optimizes the relationship between beam width and side-lobe level. *Proc.I.R.E.*, **34**, 335–348.

Haugen, J.E., 1992: Implicit normal mode schemes in the HIRLAM model. Unpublished manuscript, 26pp.

Huang, Xiang-Yu and Peter Lynch, 1993: Diabatic digital filtering initialization: application to the HIRLAM model. *Mon. Wea. Rev.*, **121**, 589–603.

Lynch, Peter and Xiang-Yu Huang, 1992: Initialization of the HIRLAM model using a digital filter. *Mon. Weather Rev.*, **120**, 1019–1034.

Lynch, Peter, 1997: The Dolph-Chebyshev Window: A Simple Optimal Filter. *Mon. Wea. Rev.*, **125**, 655-660.

Lynch, Peter, Dominique Giard and Vladimir Ivanovici, 1997: Improving the efficiency of a digital filtering scheme. *Mon. Wea. Rev.*, **125**, 1976–1982.

Machenhauer, B., 1977: On the dynamics of gravity oscillations in a shallow water model with applications to normal mode initialization. *Beitr. Atmos. Phys.*, **50**, 253–271.

Richardson, L.F., 1922: *Weather Prediction by Numerical Process.* Cambridge Univ. Press, 236 *pp.* Reprinted by Dover Publications, New York, 1965.

Temperton, C., 1988: Implicit normal mode initialization. *Mon. Wea. Rev.*, **116**, 1013–1031.

List of HIRLAM Technical Reports.

1. Gustafsson, N., Järvenoja, S., Källberg, P. and Nielsen, N.W. (1986). Baseline experiments with a high resolution limited area model. Copenhagen, November 1986.
2. Nordeng, T.E. and Foss, A. (1987). Simulations of storms within the HIRLAM baseline experiment with the Norwegian mesoscale limited area model system. Olso, March 1987.
3. Gustafsson, N. and Svensson, J. (1988). A data assimilation experiment with high resolution TOVS data. Norrköping, January 1988.
4. Myrberg, K., Koistinen, J. and Järvenoja, S. (1988). A case study of non-forecasted cyclogenesis in polar air mass over the Baltic sea. Helsinki, November 1988.
5. Machenhauer, B. (1988). HIRLAM Final Report. Copenhagen, December 1988.
6. Lynch, P. and McGrath, R. (1990). Spectral Synthesis on Rotated and Regular Grids. December 1990.
7. Kristjánsson, J.E. and Huang, X.-Y. (1990). Implementation of a consistent scheme for condensation and clouds in HIRLAM. December 1990.
8. HIRLAM Workshop on Mesoscale Modelling—Copenhagen, Denmark, 3-5 September 1990. December 1990.
9. Gustafsson, N. (1993). HIRLAM 2 Final Report. Norrköping, March 1993.
10. Lynch, P. (1993). Digital Filters for Numerical Weather Prediction. January 1993.
11. Huang, X.-Y., Cederskov, A. and Källén, E. (1993). A Comparison between Digital Filtering Initialization and Nonlinear Normal Mode Initialization in a Data Assimilation System. June 1993.
12. Lynch, P. and Huang, X.-Y., (1993). Initialization Schemes for HIRLAM based on Recursive Digital Filters. October 1993.
13. Eerola, K. (1993). Experimentation with Second and Fourth Order Horizontal Diffusion Schemes. October 1993.
14. Kristjánsson, J.E. and Thorsteinsson, S. (1994). Simulations of intense cyclones near Iceland. Norrköping, March 1994.
15. Sass, B.H. and Christensen, J.H. (1994). A Simple Framework for Testing the Quality of Atmospheric Limited Area Models. Norrköping, August 1994.
16. HIRLAM-2 Radiation Scheme: Documentation and Tests. Norrköping, November 1994.
17. McDonald, A. (1994). The HIRLAM two time level, three dimensional semi-Lagranian, semi-implicit, limited area, grid point model of the primitive equations. Norrköping, March 1995.
18. Gollvik, S., Bringfelt, B., Perov, V., Holtslag, A. A. M. (1995). Experiments with nonlocal vertical diffusion in HIRLAM. Norrköping, March 1995.
19. Bringfelt, B., Gustafsson, N., Vilmusenaho, P. and Järvenoja, S. (1995). Updating of the HIRLAM physiography and climate data base. Norrköping, June 1995.
20. Bazile, E. (1995). Study of a prognostic cloud scheme in Arpege. Norrköping, August 1995.
21. Huang, X.-Y. (1995). Initialization of cloud water content in the HIRLAM data assimilation system. Norrköping, August 1995.
22. Lönnberg, P. Observing system experiments on North Atlantic radiosondes. Norrköping, February 1996.
23. Bringfelt, B. Tests of a new land surface treatment in HIRLAM. Norrköping February 1996.
24. Lynch, P. A Simple Filter for Initialization, Norrköping, March 1996.
25. Perov, V and Gollvik, S. A 1-D Test of a Nonlocal, E-ε Boundary Layer Scheme for a NWP Model Resolution. Norrköping, April 1996.
26. Huang, X.-Y. and Yang, X. Variational Data Assimilation with the Lorenz Model. Norrköping, April 1996.
27. McDonald, A. Sources of noise in the "physics"; a preliminary study. Norrköping, November 1996.
28. Navascués, B. Analysis of 2 meter Temperature and Relative Humidity. Norrköping, January 1997.
29. Kristjánsson, J E and Thorsteinsson, S and Úlfarsson, G. Potential Vorticity Based Interpretation of the Evolution of the Greenhouse Low, 3 Feb 1991. Norrköping, January 1997.

30. Berre, L. Non-separable structure functions for the HIRLAM 3DVAR. Dublin, November, 1997.

31. Stoffelen, A. and P. van Beukering. Implementation of improved ERS scatterometer data processing and its impact on HIRLAM short range weather forecasts. Dublin, November, 1997.

32. McDonald, A. Lateral boundary conditions for operational regional forecast models; a review. Dublin, November, 1997.

33. Mogensen, K.S. and Xiang-Yu Huang. Variational Parameter Estimation with the Lorenz Model. Dublin, June, 1998.

34. McDonald, A. Alternative Extrapolations to find the Departure Point in a 'Two Time Level' Semi-Lagrangian Integration. Dublin, June, 1998.

35. Marja Bister. Cumulus Parameterisation in Regional Forecast Models: A Review. Dublin, August, 1998.

36. Thor Erik Nordeng, Lars Anders Breivik, Anstein Foss and Knut Helge Midtbø. A Simple and Efficient Method to Obtain Flow Dependent Structure Functions for Objective Analysis of Weather Elements. Dublin, August, 1998.

37. Cisco de Bruijn. Precipitation Forecasts with a Very High Resolution Version of HIRLAM for the TelFlood Project. Dublin, August, 1998.

38. Bjarne Amstrup and Xiang-Yu Huang. Impact of the Additional FASTEX Radiosonde Observations on the HIRLAM Data Assimilation and Forecasting System. Dublin, October, 1998.

39. Annica Ekman and Erland Källén. Mass Conservation Tests with the HIRLAM Semi-Lagrangian Time Integration Scheme. Dublin, December, 1998.

40. Nils Gustafsson *et al.* Three-dimensional Variational Data Assimilation for a High Resolution Limited Area Model (HIRLAM). Dublin, January, 1999.

41. Ivar Lie. Some aspects of non-hydrostatic models in the HIRLAM perspective. Dublin, May, 1999.

42. Peter Lynch, Ray McGrath and Aidan McDonald. Digital Filter Initialization for HIRLAM. Dublin, June, 1999.

43. Aidan McDonald. Well-posed Boundary Conditions for Semi-Lagrangian Schemes: The One-dimensional Case.

44. Aidan McDonald. Well-posed Boundary Conditions for Semi-Lagrangian Schemes: The One-dimensional Case, Part II.